Research Square

Preprints are preliminary reports that have not undergone peer review.
They should not be considered conclusive, used to inform clinical practice,
or referenced by the media as validated information.

Development of Solid Lipid Nanoparticles Containing Budesonide for Inflammatory Bowel Disease (IBD) Based on the Quality by Design (QbD) Approach

Mazen Al-Mohaya
mazenalmohia@gmail.com
Istanbul University
Burcu Demiralp
Istanbul University
Özlem Akbal-Dağıstan
Istanbul University
Neşet Neşetoğlu
Istanbul University
Yıldız Özsoy
Istanbul University

Research Article

Keywords: Solid lipid nanoparticles, Budesonide, In-vitro, Quality by Design, Liquisolid

Posted Date: May 11th, 2026

DOI: https://doi.org/10.21203/rs.3.rs-9118605/v1

License: This work is licensed under a Creative Commons Attribution 4.0 International License. Read Full License

Additional Declarations: No competing interests reported.

Abstract

This study aimed to develop and optimize budesonide-loaded solid lipid nanoparticles (BUD-SLNs) through a Quality by Design (QbD) framework and to assess their in vitro performance systematically. SLNs were prepared by hot homogenization, and critical formulation variables, including cetyl stearyl alcohol (CSA), Cremophor® A25 (CA25), Gelucire® 44/14 (G44), and homogenization time were optimized using a central composite design. The impact on particle size (PS), polydispersity index (PDI), entrapment efficiency (EE%), and drug release in pH 7.5 buffer after 2 hours was assessed as critical quality attributes (CQAs). Syloid® XDP 3150 was used to convert liquid SLNs into solid dosage forms, which were then capsulated in delayed-release capsules. Solubility screening identified CSA and CA25/G44 as optimal lipid and surfactant candidates. The optimized formulation exhibited a PS of 10.15 ± 0.12 nm, PDI of 0.104 ± 0.01, EE% of 99.80 ± 0.01%, and drug release of 98.53 ± 2.30% after 2 hours. In biorelevant FaSSIF/FeSSIF media, drug release reached 102.24 ± 1.7% and 108.65 ± 4.2%, respectively. DSC analysis confirmed successful drug encapsulation. In vitro lipolysis testing revealed consistent Bud release upon pancreatic enzyme addition, suggesting robust formulation integrity during digestion. The optimized BUD-SLNs showed no cytotoxicity on Caco-2 cells and retained physicochemical stability under ICH conditions. Overall, these findings highlight the potential of SLNs for enhancing the solubility and oral delivery of budesonide, supporting future translational development and preclinical application.

Introduction

Inflammatory bowel disease (IBD), comprising Crohn's disease (CD) and ulcerative colitis (UC), is a chronic, relapsing inflammatory disorder of the gastrointestinal tract that affects approximately 6.9 million individuals worldwide, with increasing prevalence in newly industrialized regions(1). UC typically involves continuous inflammation of the colonic mucosa, whereas CD presents with transmural, granulomatous inflammation affecting any segment of the GI tract in a discontinuous pattern(2). Both conditions are associated with significant morbidity, including abdominal pain, diarrhea, hematochezia, weight loss, and extraintestinal complications, impacting patients' quality of life and healthcare systems(3, 4).

Corticosteroids are frequently employed for inducing remission in moderate-to-severe CD. However, their long-term use is limited due to systemic side effects such as osteoporosis, hyperglycemia, and immune suppression(4). Budesonide (BUD) is a synthetic glucocorticoid with high topical anti-inflammatory activity and extensive first-pass metabolism. Despite complete absorption from the GI tract, BUD's oral bioavailability remains low (10–20%) due to its rapid hepatic metabolism via CYP3A4(3). Additionally, its poor aqueous solubility (28 µg/mL) and lipophilicity (log P = 3.2) classify it as a Biopharmaceutics Classification System (BCS) Class II drug, necessitating formulation strategies to enhance solubility and systemic availability(5).

Conventional BUD products, such as enteric-coated capsules (e.g. Entocort®) or enteric-coated micropellets contained in a capsule (e.g. Budenofalk®), rely on pH-dependent polymer coatings to delay drug release until the distal ileum or colon(6). However, these systems are limited by variable dissolution and low solubility of BUD in intestinal fluids. The use of lipid nanoparticles encapsulated within acid-resistant capsules offers a dual advantage of enhanced solubilization and targeted intestinal delivery.

Among various approaches to improve solubility and bioavailability, lipid-based drug delivery systems(7), especially solid lipid nanoparticles (SLNs), have emerged as promising carriers for BCS Class II drugs(8). SLNs are submicron colloidal carriers composed of a solid lipid matrix stabilized by surfactants, capable of enhancing solubility, protecting labile drugs, providing controlled release, and facilitating lymphatic uptake. They have demonstrated success in improving the pharmacokinetic profiles of several poorly soluble drugs(9, 10), including glibenclamide, gliclazide, and hydrochlorothiazide(11–13).

The performance of SLNs is strongly influenced by formulation and processing variables, including lipid type, surfactant concentration, and homogenization conditions(14). Conventional trial-and-error approaches often fail to adequately control these factors. In contrast, the Quality by Design (QbD) paradigm, endorsed by regulatory agencies such as the FDA and ICH, offers a systematic approach to formulation development by defining the Quality Target Product Profile (QTPP), identifying Critical Quality Attributes (CQAs), and optimizing formulation and process parameters through risk assessment and design of experiments (DoE)(15–17).

This study aimed to develop and optimize a formulation of BUD-loaded SLNs using a QbD framework to enhance the oral bioavailability and therapeutic performance of BUD, primarily through improved solubility, protection against gastrointestinal degradation, and lymphatic delivery to avoid first-pass metabolism. Critical formulation factors were identified and optimized using a central composite design, and the final formulation was characterized for particle size, polydispersity index (PDI), entrapment efficiency (EE%), and in vitro drug release. The study also evaluated solidification strategy, biorelevant dissolution behavior, and cytotoxicity to ensure the biocompatibility and safety of the developed SLNs and their excipients on intestinal epithelial cells (Caco-2), confirming suitability for oral administration.

Materials and Methods

Materials

BUD was obtained from Aartı Industries (India). Cutina® CP, Kolliwax® S, Novata® BCF PH, Novata® B PH, and Tween 80 were kindly gifted from BASF (Germany). Cetyl Stearyl Alcohol was supplied by Ataman Kimya A.Ş. (Turkey). Compritol® 888 ATO, Compritol® E ATO, Precirol® ATO 5, Geleol™, Gelucire® 44/14, Gelucire® 48/16, and Transcutol P® were graciously provided by Gattefosse (France). Pluronic® F68, Pluronic® F-127, and Cremophor® A25 were sourced from Sigma-Aldrich (Germany). Neusilin UFL2® and Neusilin US2® were kindly provided by Fuji Chemical (Japan). Florite® R and Florite® PS-200 were from Tomita Pharmaceutical (Japan). Syloid® XDP 3050 and Syloid® XDP 3150 were received from Grace (USA). EMBOCAPS® AP (capsules) was kindly gifted by Suheung America Corporation (Korea). 3F Powder™, FaSSIF, and FeSSIF Buffer Concentrate were purchased from Biorelevant (UK). Bile bovine, Pancreatin from porcine pancreas (≥ 3 x USP specifications, pancreatic extract), 4-bromophenylboronic acid (4-BBBA), and Trizma® maleate were

purchased from Sigma-Aldrich (Germany). Lipoid S100 was purchased from Lipoid (Germany). All reagents were of analytical grade and used without further purification.

Solubility by Equilibrium Method

The equilibrium solubility of BUD was determined in buffer solutions (pH 1.2, 4.5, and 6.8) and in biorelevant media (FaSSIF/FeSSIF). Excess BUD powder (9 mg) was added to 1 mL of each medium in Eppendorf tubes to achieve supersaturation, as indicated by visible precipitate. Samples were incubated in an orbital shaker (Model 420, Thermo Electron Corporation) at 37.0 ± 0.5°C and 150 rpm for 24 h (18, 19). After equilibration, the suspensions were centrifuged (15,000 rpm, 15 min, Model D-7200, Hettich, Germany), and 100 µL of supernatant was diluted to 10 mL with the mobile phase. The solutions were filtered through 0.45 µm regenerated cellulose membrane filters (Sartorius, Germany) and analyzed by HPLC. The dose-to-solubility ratio (D_0) was calculated using Eq.

$D_0 = \frac{Dose/s}{250mL}$ (1)

Where Dose is the highest prescribed oral dose (mg) and S is the equilibrium solubility (mg/mL). According to FDA guidelines, a compound is classified as highly soluble when $D_0 \leq 1$ under these conditions(20).

Solubility Studies

The solubility of BUD was assessed in various lipids (Cutina® CP, Cetyl Stearyl Alcohol, Compritol® 888 ATO, Compritol® E ATO, Precirol® ATO 5, Geleol™, Kolliwax® S, Novata® BCF PH, and Novata® B PH) and surfactants/co-surfactants (Pluronic F68, Cremophor® A25, Pluronic® F-127, Gelucire® 44/14, Gelucire® 48/16, Tween 80, and Transcutol P®). The test tube equilibrium method was employed, in which 1g of each lipid was heated to 5°C above its melting point. BUD was added incrementally in 1mg until complete dissolution. Solubility was visually confirmed and quantified as mg of BUD dissolved per gram of lipid, following published procedures(21).

Quality by Design (QbD) Approach

The QbD approach was implemented to define the QTPP, CQAs, Critical Material Attributes (CMAs), and Critical Process Parameters (CPPs)(15). Risk assessment was conducted using Failure Mode and Effects Analysis (FMEA) to prioritize variables influencing CQAs, followed by Design of Experiments (DoE) to optimize process and formulation conditions(22).

Preliminary Studies

Formulation variables were screened based on QTPP and solubility outcomes. Cetyl Stearyl Alcohol was selected as a lipid, and Cremophor® A25 and Gelucire® 44/14 were identified as suitable surfactants. Selection was also guided by desired particle size and PDI values(23).

Preparation of BUD-SLNs

SLNs were prepared by hot homogenization. The solid lipid was melted at 10°C above its melting point, and BUD was dispersed in the lipid phase. An aqueous surfactant phase, preheated to the same temperature, was added to the lipid phase and homogenized (Ultra-Turrax T25, IKA, Germany) at 10,000 rpm for varied durations. Formulations were cooled to room temperature to obtain nanoparticles(24).

DoE for BUD-SLNs

Experimental design methodologies were applied to optimize the formulation and achieve the predefined QTPP. Within the QbD framework, the critical elements-QTPP, CQAs, CPPs, and CMAs were systematically established. Preliminary formulation experiments, supported by literature review and risk assessment, facilitated the identification of variables exerting a significant impact on product quality(25). Among these, lipid concentration, surfactant concentration, and homogenization time were identified as the most influential parameters affecting the performance of BUD-SLNs. For formulation optimization, four independent variables were selected (lipid concentration, two surfactant concentrations, and homogenization time), while four dependent variables, particle size (PS), polydispersity index (PDI), entrapment efficiency (EE%), and cumulative drug release after 2 hours (%) were defined as CQAs. A central composite design (CCD), a response surface methodology (RSM), was employed to systematically evaluate the main, interaction, and quadratic effects of these independent variables on the CQAs. The CCD incorporated two factor levels (-1 and + 1) with three replicates at the center point to ensure robustness of the statistical model. Optimization and analysis of the experimental data were carried out using Minitab® 20.2 software, enabling the identification of optimal process and formulation conditions.

Characterization of BUD-SLNs

Particle Size (PS) and Polydispersity Index (PDI)

Measured at 25°C using a Malvern ZetaSizer (1000 HS, UK) after 10-fold dilution with distilled water. Results reported as mean Z-average (d.nm) ± SD(26).

Zeta Potential (ZP)

Determined using a Malvern ZetaSizer (1000 HS, UK) with 10-fold diluted samples in folded capillary zeta cells (DTS1070). Results expressed as mean ZP (mV) ± SD(27).

Entrapment Efficiency (EE%)

About 1 mL of the BUD-SLN dispersion was placed in a tube and centrifuged (25,000 rpm, 30 min, Hettich D-7200, Germany). The quantification of free drug (BUD) in the supernatant by HPLC(28). The EE% was calculated using Eq. (2):

$$EE\% = \frac{W_{initial} - W_{free}}{W_{initial}} \quad (2)$$

Where $W_{initial}$ drug is amount of BUD added in the formulation, and W_{free} drug is the amount of BUD in supernatant.

Solidification of Liquid BUD-SLNs

The liquisolid technique was used to adsorb liquid BUD-SLNs onto solid carriers (Florite® R, Florite® PS-200, Neusilin® US2, Neusilin® UFL2, Syloid® XDP 3050, Syloid® XDP 3150). Mixtures were stirred, dried at room temperature for 24 h, and optimized for free-flowing powder suitable for capsule filling(29).

Powder Flow Properties

Bulk and tapped density, Carr's Index, Hausner's ratio, and angle of repose (θ) were determined using pharmacopeial methods for BUD-SLNs and pure BUD powders(30). Measurements were performed in triplicate.

Differential Scanning Calorimetry (DSC)

Thermal properties of BUD and optimized SLNs were analyzed using a DSC-60 (Shimadzu, Japan). Approximately 5 mg of each sample was sealed in aluminum pans and scanned from 20–300°C at 10°C/min.

In Vitro Drug Release Study

The dissolution profiles of capsulated BUD-SLN formulations and a marketed product were evaluated using a USP Dissolution Apparatus II (paddle method) in accordance with FDA-recommended protocols. Capsules were placed in sinkers and immersed in 1000 mL of dissolution medium at 37 ± 0.5°C, with a paddle speed of 75 rpm. Two dissolution media were employed: (i) 0.1 N HCl (pH 1.2 ± 0.05) to simulate gastric conditions, and (ii) phosphate buffered saline (pH 7.5 ± 0.05) to simulate intestinal fluid. Additionally, the optimized capsulated BUD-SLN formulation was evaluated in biorelevant media, FaSSIF (pH 6.5 ± 0.05) and FeSSIF (pH 5.0 ± 0.05), to simulate fasted and fed states, respectively. Sampling was performed at 2-hour intervals in acidic medium and at 0.25, 0.5, 1, 2, 4, 6, and 8 hours in buffer and biorelevant media. At each time point, 3 mL aliquots were withdrawn, filtered, and replaced with equal volumes of fresh dissolution medium to maintain sink conditions. Filtration was carried out using RC filters (0.45 µm, Sartorius, Germany) for acid-base media and polypropylene/glass microfiber filters (0.45 µm, Biorelevant, UK) for FaSSIF/FeSSIF. BUD concentration in dissolution samples was quantified by HPLC (Shimadzu LC 20-AT, Japan) following the USP method for budesonide (USP, 2014) and validated according to ICH Q2 guidelines. Chromatographic separation was achieved using a BDS HYPERSIL C18 column (4.6 × 100 mm, 3 µm, Thermo Scientific™, USA) with a mobile phase consisting of sodium phosphate buffer (pH 3.2 ± 0.05) and acetonitrile (68:32, v/v). The column temperature was maintained at 25°C, with a flow rate of 1.5 mL/min, an injection volume of 50 µL, and UV detection at 254 nm.

In Vitro Lipolysis Study

The *in vitro* lipolysis study was performed with modifications to the method reported by Nazlı et al. (31). A lipolysis buffer (pH 6.5 ± 0.05) was prepared to simulate the intestinal environment under fasting conditions. The buffer contained 2 mM Tris-maleate, 1.4 mM $CaCl_2 \cdot 2H_2O$, 50 mM NaCl, 2.95 mM bile salts, and 0.26 mM Lipoid S100. The pH was adjusted to 6.5 with NaOH or HCl. The experiment was conducted at 37°C in two stages: a dispersion phase and a digestion phase. During dispersion, the optimized BUD-SLN formulation was introduced into the lipolysis medium and allowed to equilibrate for 15 minutes. The pancreatic lipase extract was freshly prepared before each experiment by dispersing 1 g of porcine pancreatin powder in 5 mL of lipolysis buffer (without bile salts and phospholipids). The mixture was stirred for 15 minutes, centrifuged at 4000 rpm for 15 minutes, and the supernatant was adjusted to pH 6.5. Fresh extract was used to minimize enzyme activity loss. At the end of the dispersion phase, the extract was added to initiate the digestion phase. The medium's pH was maintained at 6.5 ± 0.05 using 0.4 M NaOH titration, which was not included in volume calculations. Samples were withdrawn at 10 and 15 minutes during dispersion and at 5, 15, 30, 45, and 60 minutes during digestion. To quench lipase activity immediately, 50 µL of 4-bromophenylboronic acid (4-BBBA) was added to each sample. The samples were then centrifuged at 4000 rpm for 30 minutes, and the concentration of BUD in the aqueous supernatant was determined using a validated HPLC method.

In Vitro Cytotoxicity Studies

The cytotoxicity of the optimized BUD-SLN formulations was evaluated using the MTT assay, which measures the conversion of yellow MTT to purple formazan crystals by mitochondrial dehydrogenases of viable cells, as previously described by Hussain et al.(32). Human colorectal adenocarcinoma Caco-2 cells (ATCC HTB-37) were cultured in EMEM supplemented with 5% fetal bovine serum (FBS), 100 U/mL penicillin, and 100 µg/mL streptomycin (all from Sigma-Aldrich). Cells were seeded in 96-well plates (4×10^4 cells/well) and incubated for 24 h at 37°C in a humidified atmosphere containing 5% CO_2. After attachment, the medium was replaced with serum-free medium containing either (i) liquid-optimized BUD-SLNs, (ii) powder-optimized BUD-SLNs, (iii) pure BUD (positive control), or (iv) drug-free SLNs (negative controls). A control group of untreated cells (medium only) was included. Cells were further incubated for 24, 48, or 72 h under the same conditions. At the end of each incubation period, the medium was replaced with 30 µL/well of MTT solution (5 mg/mL in PBS) and incubated for 4 h at 37°C. The MTT solution was then carefully aspirated, and 100 µL/well of DMSO was added to dissolve the formed formazan crystals. Plates were shaken at room temperature for 2 h to ensure complete solubilization. Absorbance was measured at 570 nm (reference 600 nm) using

a Bio-Tek microplate reader (Bio-Tek Instruments, Germany). Triton X-100 was included as a positive control for cytotoxicity. Each experiment was performed in triplicate on at least three independent occasions. Results are expressed as the percentage of viable cells relative to the untreated control group.

Stability Studies

The optimized BUD-SLNs were stored in amber glass bottles under ICH stability conditions (25 ± 2°C/65 ± 5% RH and 40 ± 2°C/75 ± 5% RH). Samples were analyzed for PS, PDI, EE%, and drug release at 0, 1, 2, and 3 months(33).

Statistical Analysis

Statistical analyses were performed using Minitab® 20.2 (Minitab Inc., USA), and graphical data visualization was carried out in Microsoft Excel 2010 (Microsoft Corp., USA). All results are expressed as mean ±standard deviation (SD) from at least three independent experiments (n = 3). Statistical significance was set at $p < 0.05$. For optimization studies, overall desirability (D) was calculated, ranging from 0 (undesirable) to 1 (optimal). For cytotoxicity evaluations, statistical differences between treatment groups and controls were assessed using one-way analysis of variance (ANOVA) followed by pairwise t-tests. Results were annotated as $^{***}p \leq 0.0001$ compared with the liquid formulation control and $^{\#\#\#}p \leq 0.0001$ compared with the powder formulation control.

Results

Solubility by Equilibrium Method

Table 1 presents the solubility results, dose-to-solubility ratio, and dose number (D_0) for BUD. The maximum dose strength for BUD is 9 mg. The equilibrium solubility method showed that BUD exhibits low solubility across all buffer solutions (pH 1.2, 4.5, and 6.8), with no significant improvement in solubility across the pH range. The dose-to-solubility ratio in all buffers exceeded 250 mL, resulting in D_0 values greater than 1. The lowest solubility was observed at pH 6.8.

Solubility Studies

Lipids: BUD solubility was highest in Cetyl Stearyl Alcohol (~ 21 ± 1 mg/g), followed by Geleol™ (~ 11 ± 1.5 mg/g), Kolliwax® S (~ 10 ± 0 mg/g), and Precirol® ATO 5 (~ 5 ± 1.2 mg/g), as shown in Fig. 1(a). Surfactants: Solubility was highest in Transcutol P® (~ 44 ± 2 mg/g), followed by Cremophor® A25 (~ 23 ± 2.3 mg/g), Gelucire® 44/14 (~ 17 ± 1.2 mg/g), Gelucire® 48/16 (~ 12 ± 2 mg/g), and Tween 80 (~ 12 ± 1.1 mg/g), as presented in Fig. 1(b). Based on solubility data and formulation suitability, Cetyl Stearyl Alcohol (CSA) was selected as the lipid, and Cremophor® A25 (CA25) and Gelucire® 44/14 (G44) as surfactants for SLN development.

Evaluation and Selection of Solidification Adsorbents for BUD-SLNs

For size 0 capsules, an optimal powder density of 0.6–1.2 g/mL is required to achieve fill weights between 408–816 mg. Among the tested excipients, Syloid® XDP 3050 and Syloid® XDP 3150 demonstrated the most favorable flow characteristics, with low Hausner ratios (1.2), Carr's Index values (14.3–17.2%), and an angle of repose (26°). Both produced free-flowing powders that filled capsules adequately without the need for additional flow enhancers. Syloid® XDP 3150 was further selected for subsequent studies based on its consistent drug release profile (data not shown). The optimized BUD-SLNs:Syloid® XDP 3150 (1:0.1 g) formulation exhibited a bulk density of 0.59 g/mL, Hausner ratio of 1.0, and Carr's Index of 3.3%, indicative of excellent compressibility and minimal cohesiveness. In contrast, Florite® R and Florite® PS-200 showed poor flowability, characterized by high Hausner ratios, high Carr's Index values, and large angles of repose. Neusilin® US2 and Neusilin® UFL2 displayed moderate flow properties, although Neusilin® US2 performed slightly better than Neusilin® UFL2. Pure BUD exhibited very poor flowability, with a high Hausner ratio and Carr's Index, confirming strong aggregation tendencies, as shown in Table S1. Based on these findings, Syloid® XDP 3150 was identified as the most suitable adsorbent for solidifying BUD-SLNs, ensuring optimal flowability, appropriate capsule density, and stable release performance.

QbD Approach and Preliminary Studies

The QTPP was established as the first step in the QbD approach. A comprehensive QTPP profile for BUD-loaded SLNs was developed using prior knowledge, preliminary experimentation, and published reports, as presented in Table S2. From the QTPP, CQAs were identified and their criticality was justified, as illustrated in Table 2. The selected CQAs included PS, PDI, EE%, and drug release after 2 hours in pH 7.5 buffer, as these parameters directly influence in vivo performance, safety, and efficacy.

CPPs and CMAs relevant to the hot homogenization process were determined through initial risk assessment, as presented in Table S3. CMAs included the ratio of CSA as solid lipid and CA25 and/or G44/14 as surfactants, while homogenization time (HT) was identified as the key CPP. Their relevance to the BUD-SLN formulation warranted further evaluation. These findings guided the subsequent optimization of formulation variables to achieve the desired QTPP.

DoE for BUD-SLNs

CCD was applied for the optimization of BUD-SLNs using four independent variables (CSA concentration, CA25 concentration, G44 concentration, and homogenization time), four dependent variables (PS, PDI, EE%, and cumulative drug release after 2 h), and two controlled variables (temperature and homogenization speed). Minitab® 20.2 software generated 27 runs, as shown in Tables 3 and 4.

The PS (Y1) remained consistent across most runs, ranging from 10–11 nm (± 0.02 to ± 0.60). A single outlier of 54.90 ± 68.90 nm was observed. The PDI (Y2) values ranged between 0.07 and 0.25, remaining within acceptable limits for nanoparticle formulations. EE% (Y3) demonstrated very high uniformity,

with values between 99.8–99.9% and minimal standard deviation. The cumulative drug release after 2 h (Y4) varied more widely, with values ranging from 58.48% to > 100%.

Increasing lipid concentration from 10% to 15%, while varying surfactant concentration and homogenization time, did not significantly affect PS, PDI, or EE%. In two formulations (runs 8 and 16), signs of gelation were observed.

Regression analysis was performed to evaluate model fit for each response. The PS model showed R^2=78.78% (S = 0.733), but adjusted R^2 dropped to 49.07%, and predicted R^2=0.00%. The PDI model showed R^2=71.57% (S = 0.466), adjusted R^2=31.77%, and predicted R^2=0.00%. The EE% model achieved R^2=77.00% (S = 0.03), with adjusted R^2=44.81% and predicted R^2=0.00%. The drug release model demonstrated R^2=78.31% (S = 9.80), adjusted R^2=47.92%, and predicted R^2=0.00%. Collectively, these models demonstrated moderate to strong explanatory power but poor predictive capability.

Effect of Independent Variables on PS

The 3D surface plot illustrates the relationship between HT and CA25 concentration on PS while holding CSA (15%) and G44 (0%) constant. The response surface shows a nonlinear interaction, where PS decreases with increasing HT but rises again at longer durations, forming a U-shaped trend. The influence of CA25 is minimal at lower HTs but becomes more pronounced at extended durations. The normal plot of standardized effects indicated that the quadratic term of HT (DD) had a statistically significant positive effect on PS, while other factors were not significant, as seen in Figs. 2 and 3(a).

Effect of Independent Variables on PDI

The 3D surface plot shows that HT and CA25 concentration influence the PDI. Increased HT and higher CA25 concentrations led to higher PDI values, suggesting reduced uniformity. The normal plot highlighted the significant positive interaction effect between CSA (A) and CA25 (B) (AB), as shown in Figs. 2 and 3(b).

Effect of Independent Variables on EE%

The 3D surface plot shows that both HT and CA25 concentration affect EE% non-linearly. At lower CA25 concentrations, EE% was higher, but values declined as CA25 increased, before slightly rising again. Shorter HT favored higher EE%, while longer HT reduced it. The normal plot of standardized effects indicated significant positive contributions from G44 concentration (C), CSA × G44 interaction (AC), and the quadratic term of CA25 (BB), as seen in Figs. 2 and 3(c).

Effect of Independent Variables on Cumulative Drug Release

The 3D surface plot shows that cumulative drug release after 2 h increased initially with HT and CA25 concentration but plateaued or decreased at higher values. The normal plot of standardized effects indicated that square HT (DD) had a positive effect, while square CA25 (BB) had a negative effect, as seen in Figs. 2 and 3(d).

Validation of the Mathematical Model

Optimization of BUD-SLNs was validated using Minitab®'s Response Optimizer. A checkpoint batch (run 4) was prepared and compared against predicted values. A t-test indicated no significant difference ($p > 0.05$). The model achieved a desirability value of 0.9506, suggesting a robust design, as presented in Table 5.

Characterization of Optimized BUD-SLNs (dup: abstract ?)

Particle Size (PS) and Polydispersity Index (PDI) Determination

The optimized liquid BUD-SLNs exhibited a mean PS of 10.15 ± 0.12 nm. The PDI was found to be 0.104 ± 0.01, indicating a narrow size distribution, as seen in Figure S1.

Zeta Potential (ZP)

The optimized liquid BUD-SLNs exhibited a ZP of − 3.89 ± 0.82 mV.

Entrapment Efficiency (EE%)

The optimized liquid BUD-SLNs demonstrated an EE% of 99.80 ± 0.01%.

Differential Scanning Calorimetry (DSC)

The DSC thermogram of pure BUD showed a distinct endothermic peak at 257.89°C. In the optimized BUD-SLNs, this peak disappeared, and a single sharp endothermic peak at ~ 44.24°C was observed, corresponding to CSA, as illustrated in Figure S2.

In Vitro Drug Release Study

The dissolution study demonstrated that no drug release occurred from the BUD-SLNs at a pH of 1.2, indicating that the capsules remained intact in acidic conditions. The capsule completely disintegrated, releasing the filled optimized solidified BUD-SLNs in basic conditions. The dissolution study in PBS (pH 7.5

± 0.05) showed a rapid and nearly complete drug release, with 98.53 ± 2.30% of BUD released within 2 hours, as shown in Fig. 4(a). In contrast, the marketed product exhibited a slower, sustained release profile, with 55.7% ±1.4% of the drug released within 2 hours.

The optimized solidified BUD-SLNs formulation demonstrated rapid and complete drug release in both FaSSIF and FeSSIF, as shown in Fig. 4(b). In FaSSIF, the formulation achieved a cumulative drug release of approximately 102.24 ± 1.7% within 2 hours, plateauing thereafter and maintaining a high release profile throughout the 8-hour period. In FeSSIF, drug release was slightly higher, reaching up to 108.65 ± 4.2%. In contrast, the marketed product exhibited no detectable drug release in either FaSSIF or FeSSIF throughout the study duration.

In Vitro Lipolysis Study

The optimized BUD-SLNs formulation (3mg, ~ 100% drug load) was evaluated using an in-vitro lipolysis model designed to simulate the digestion of lipid-based drug delivery systems in the gastrointestinal tract. To evaluate drug distribution, the lipolysate was centrifuged, and under fasted conditions, the aqueous phase demonstrated a high solubilization capacity for BUD, reaching approximately 105%. These results highlight the effective digestion and solubilisation of the optimized BUD-SLNs in simulated gastrointestinal conditions. The percentage of BUD dissolved in the aqueous phase increased slightly after the onset of digestion, with no significant impact observed from the hydrolysis of excipients. The digestion process was rapid, completing within 60 minutes, as shown in Fig. 4(c), which illustrates the BUD dissolved percentage at a constant pH of 6.5 ± 0.05.

In Vitro Cytotoxicity Studies

The IC_{50} value of BUD in the Caco-2 cell line was calculated to be 59.81 µM, as seen in Figure S3(a and b). There was no statistically significant difference ($p \leq 0.001$) in the effect on cell viability between optimized solidified BUD-SLNs formulation and optimized liquid BUD-SLNs. For the placebo (drug-free) liquid formulation, cell viability at 24, 48, and 72 hours was 99.87%, 95.32%, and 93.26%, respectively; for the solidified formulation, these values were 99.79%, 95.28%, and 93.36%. In the drug-containing liquid formulation, cell viability at 24, 48, and 72 hours was 89.24%, 85.62%, and 81.68%, respectively; for the solidified form, the values were 88.79%, 82.35%, and 79.93%. Consequently, it was determined that both the drug-containing and placebo optimized solidified BUD-SLNs formulation and optimized liquid BUD-SLNs are non-cytotoxic.

Stability Studies

As presented in Table 6, the optimized BUD-SLNs exhibit no significant changes in CQAs such as PS, PDI, EE%, and cumulative drug release after 2 hours at storage conditions of 25 ± 2°C / 65 ± 5% RH and 40 ± 2°C / 75 ± 5% RH.

Discussion

Solubility by Equilibrium Method

The solubility results confirm that BUD does not meet the FDA criteria for high solubility, which requires the highest dose to dissolve in ≤ 250 mL of aqueous media across pH 1.2–7.5 at 37°C. Similarly, the EMA considers the pH range 1.2–6.8, within which BUD also fails to qualify as highly soluble(34). This aligns with earlier reports describing BUD as a poorly soluble compound with solubility values around 28 µg/mL in aqueous media(5, 35, 36). The markedly lower solubility at pH 6.8 may be attributed to the weakly basic nature of BUD and its poor ionization in near-neutral to basic environments, which significantly limits dissolution in the distal intestine(37). This poor solubility, coupled with BUD's extensive first-pass metabolism, results in an oral bioavailability of only ~ 10–20%(3, 5). Such pharmacokinetic variability is clinically important, as it may contribute to inconsistent therapeutic outcomes, particularly in the management of IBD. Importantly, there are currently no published studies on BUD solubility under biorelevant conditions. This instability further complicates oral delivery, as it may exacerbate variability in systemic exposure. Collectively, these findings underscore the necessity of adopting formulation strategies aimed at enhancing solubility, stability, and bioavailability. Among the available approaches, lipid-based nanoparticles such as SLNs have shown promise in improving solubility and protecting labile drugs from gastrointestinal degradation(9–11, 24, 33).

Solubility Studies

The solubility of BUD in various lipids was evaluated as the initial step in selecting an appropriate lipid for SLN formulation. The solubility of BUD in the lipid matrix significantly influences the entrapment efficiency of SLNs(38), while surfactants impact solubility, drug release, and permeability(39). The high solubility of BUD in CSA (HLB = 16), Geleol™ (HLB = 3), and Precirol® ATO 5 (HLB = 1) suggests that solubility decreases with lower HLB values. Lipids with lower HLB values are more lipophilic, whereas higher HLB values indicate hydrophilic characteristics(40). Therefore, lipids with higher HLB values are more suitable for the solubility of hydrophobic BUD. Based on the solubility results, CSA was selected for SLN formulation. The high solubility of BUD in these surfactants is influenced by their HLB values, with CA25 (HLB = 15–17), G44 (HLB = 14), Gelucire® 48/16 (HLB = 16), and Tween 80 (HLB = 15) exhibiting solubility around an HLB of 15. Based on these findings, CA25 and G44 were selected as the surfactants for SLN formulation. However, Transcutol® P is not commonly used in oral delivery SLN. This is consistent with the literature(41).

Evaluation and Selection of Solidification Adsorbents for BUD-SLNs

The transformation of liquid BUD-SLNs into a powder form for oral use is essential for enhancing flowability, stability, and processability in pharmaceutical applications. The choice of an appropriate solidification adsorbent plays a critical role in ensuring uniformity and performance in the final formulation. Various excipients were evaluated based on bulk density, tapped density, Hausner ratio, Carr's Index, and angle of repose to determine their suitability for capsule filling(42, 43). Tan et al. (2013) reviewed solid carriers for lipid-based systems and highlighted that porous silicas such as Syloid® enhance

flowability and compressibility while maintaining high drug loading, making them particularly advantageous for transforming liquid lipid systems into solid dosage forms(44). Similarly, Patra et al. (2025) emphasized that Syloid® grades (e.g., Syloid® 244FP, XDP series) improve powder handling and stability compared to Florite® and Neusilin®, which can exhibit poor flow and sticky behavior(45). In contrast, Lin et al. (2023) reported that Neusilin® can improve flow when used in spray-dried composites, but its performance is variable, and stickiness may still occur depending on lipid ratios(46). Aldosari (2018) also evaluated Florite®, Neusilin®, and Syloid®, showing that Syloid® carriers supported superior capsule filling due to optimal bulk density and compressibility(47).

QbD Approach and Preliminary Studies

The QTPP was established as the first step in the QbD approach. Elements of the QTPP were identified based on regulatory guidance documents from ICH, FDA, and EMA, which primarily address solid oral dosage forms but were adapted for application to nanoformulations(48). A comprehensive QTPP profile for BUD-loaded SLNs was developed using prior knowledge, preliminary experimentation, and published reports. The selected CQAs included PS, PDI, EE%, and drug release after 2 hours in pH 7.5 buffer, as these parameters directly influence in vivo performance, safety, and efficacy(15). Even though the impact of these variables on SLN performance has been widely reported(15, 49), their relevance to the BUD-SLN formulation warranted further evaluation. Initial analysis highlighted lipid and surfactant concentrations as the most critical factors influencing the CQAs. For example, higher lipid concentrations increased EE% but risked elevating PS beyond the acceptable range, necessitating a balance between entrapment and particle size(21). These findings guided the subsequent optimization of formulation variables to achieve the desired QTPP.

DoE for BUD-SLNs

The CCD-based optimization revealed consistent particle sizes of 10–11 nm for most formulations, highlighting the robustness of the hot homogenization process for producing nanoscale particles. Such small particle sizes are advantageous for increasing drug dissolution, surface area, and absorption across the gastrointestinal tract, consistent with prior studies on SLNs(50). The occurrence of an outlier (54.90 ± 68.90 nm) suggests potential instability, likely due to nanoparticle aggregation, a known challenge in lipid-based systems where hydrophobic interactions and surfactant imbalance can disrupt dispersion stability(51).

The PDI values (0.07–0.25) remained within acceptable limits, supporting uniformity in particle distribution. Literature indicates that PDI values < 0.3 reflect monodispersity, which is essential for reproducibility and predictable pharmacokinetics(52).

Similarly, the exceptionally high EE% (99.8–99.9%) aligns with reports on lipophilic drugs like BUD, where lipid matrices enable efficient drug entrapment(53).

Variability in drug release (58->100%) highlights the influence of lipid-surfactant balance. High surfactant concentrations can lead to burst release, while excessive lipid content may restrict drug diffusion. This phenomenon has been described in other SLN systems, where optimal ratios are essential for maintaining controlled release. The gelation observed in runs 8 and 16 further supports that exceeding the system's lipid-surfactant tolerance can result in colloidal instability, as previously reported in lipid-based nanoparticle formulations(54).

The regression models showed moderate explanatory power but no predictive ability (R^2(pred) = 0.00%), a common limitation in DoE optimization when non-contributing variables are included. Similar outcomes have been reported in nanoparticle optimization studies, where overfitting reduces generalizability despite apparent model strength. Refinement of predictor variables and expansion of the design space could improve model performance.

Taken together, the results confirm that BUD-SLNs can be reproducibly prepared with high encapsulation efficiency and nanoscale size. However, careful optimization of lipid-surfactant ratios is required to prevent aggregation and ensure controlled release, which are critical for enhancing therapeutic consistency.

The optimization of BUD-SLNs revealed distinct influences of lipid, surfactant, and process parameters on CQAs. For PS, the quadratic effect of HT was significant, indicating that prolonged homogenization promoted aggregation, consistent with previous nanoparticle studies where excessive shear increased particle size(55).

PDI trends demonstrated that uniformity was compromised by higher surfactant concentrations and extended HT, reinforcing reports that lipid-surfactant interactions critically affect colloidal stability(56).

EE% findings highlighted that the excessive HT may lead to instability or possible leakage of the drug from the nanoparticles(57). The importance of adding G44 and its interaction with CSA aligns with studies showing that surfactants enhance encapsulation by stabilizing drug-lipid interactions(58).

Drug release results demonstrated that both HT and CA25 concentration must be carefully optimized. Moderate levels promoted rapid and complete drug release, while excessive values reduced performance, likely due to structural rearrangements, aggregation, premature drug leakage and/or altered drug release kinetics(59). Similar release behaviors have been observed in other SLN-based formulations, underscoring the importance of balancing processing conditions with lipid-surfactant ratios.

Model validation confirmed the reliability of the optimized formulation, with no significant difference between predicted and experimental values(60) and a high desirability index (> 0.95). This demonstrates that the QbD approach successfully identified robust operating conditions for BUD-SLN development.

Characterization of Optimized BUD-SLNs

The obtained particle size (10.15 nm) is well below 200 nm, which falls within the nanoscale range and aligns with the QTPP requirements for BUD-SLNs. According to the QTPP, the PS of nanoparticles should be less than 200 nm to enhance dissolution, absorption, and permeation through the gastrointestinal epithelial lining, ultimately improving bioavailability. The low PDI (0.104) confirms a monodisperse system, which is essential for ensuring stability and reproducibility in nanoparticle formulations(52).

The near-neutral ZP (− 3.89 mV) reflects the influence of negatively charged excipients. Nanoparticles with ZP values between − 10 mV and + 10 mV are generally considered approximately neutral. Such near-neutral zeta potential values may influence the colloidal stability of the nanoparticles, as they may not provide sufficient electrostatic repulsion to prevent aggregation(61, 62).

This high EE% (99.8%) can be attributed to the physicochemical properties of BUD, which is classified as a BCS Class II drug, characterized by low aqueous solubility and high permeability. Specifically, BUD exhibits a log P value of 3.2, indicating its lipophilic nature(3, 5, 63). The lipophilicity of BUD facilitates its incorporation into the lipid matrix of the nanoparticles, leading to the observed high EE%. This is consistent with previous literature(53, 64, 65).

Pure BUD exhibited a distinct endothermic peak consistent with its reported melting point (66). This characteristic peak completely disappeared in the thermogram of the optimized BUD-SLNs, indicating successful encapsulation and molecular dispersion of the drug within the lipid matrix. The DSC thermogram of the formulation displayed a single sharp endothermic peak at approximately 44.24°C, corresponding to CSA, the lipid carrier. This thermal profile suggests the solubilized state within the lipid matrix(33).

The absence of drug release at pH 1.2 confirms that the selected capsules effectively resisted gastric disintegration, thereby protecting the drug from the harsh gastric environment. The formulation employed Embocaps Acid Protection Capsules, which eliminates the need for post-filling coating processes, reducing both manufacturing costs and processing time(67). The optimized solidified BUD-SLNs exhibited an enhanced dissolution rate and solubility, attributed to nanosizing and lipid-based formulation, facilitating faster systemic absorption and improved bioavailability(9–13, 24, 33, 59). In contrast, the marketed product is designed with an enteric polymeric formulation that facilitates a controlled and gradual drug release in buffered conditions. This formulation provides approximately 75% drug release at the 6-hour mark, after which it plateaued. This is consistent with the literature(29).

The biorelevant media results emphasize the superior dissolution of optimized SLNs under both conditions. However, drug release was slightly higher in FeSSIF, suggesting that the presence of bile salts and lipids in the fed state may further facilitate solubilization of the lipid-based nanoparticle formulation. The rapid dissolution indicates that the nanosizing and lipid-based nanoparticles formulation significantly enhances drug solubility and dissolution rate, potentially leading to improved absorption and bioavailability *in vivo*. In contrast, the marketed product displayed no noticeable drug release in either FaSSIF or FeSSIF during the study. The marketed product (enteric-coated) is composed of polymeric acids, and their dissolution is significantly influenced by the pH and buffer capacity of the dissolution medium. The marketed product is designed to release BUD specifically at the high pH (> 7.0) levels found in the distal ileum or colon, and this release occurs under highly buffered conditions(6).

In vitro lipolysis confirmed efficient digestion of the lipid matrix and sustained solubilization of BUD in the aqueous phase, ensuring stability during enzymatic hydrolysis(31). The absence of a sharp decline in BUD concentration post-enzyme addition indicates that the lipid (CSA) and surfactant (CA25) together confer enzymatic stability to the SLNs. This stability helps preserve drug content and enhances the likelihood of improved bioavailability upon oral administration.

Cytotoxicity studies demonstrated that both liquid and solid SLN formulations are biocompatible, with viability above the 80% threshold considered safe(68, 69). This aligns with prior reports on SLNs as safe oral delivery systems.

The stability study findings are consistent with the established QTPP. Therefore, it can be concluded that the optimized BUD-SLNs maintain stability for up to 3 months under both conditions(33, 59).

Conclusion

This study successfully employed a Quality by Design (QbD) approach to develop and optimize solid lipid nanoparticles (SLNs) encapsulating budesonide, a poorly water-soluble corticosteroid. Through systematic design of experiments, key formulation parameters, including lipid and surfactant concentrations and homogenization time were optimized to yield nanoparticles with desirable critical quality attributes. The optimized BUD-SLNs demonstrated a uniform nano-sized particle size, low polydispersity index, high entrapment efficiency, and enhanced drug release under both phosphate buffer and biorelevant media. In vitro lipolysis confirmed the formulation's robustness during gastrointestinal digestion, and cytotoxicity testing confirmed the non-toxic nature of both liquid and solid forms. Thermal analysis and stability studies further confirmed the structural integrity and physical stability of the formulation. Collectively, these results highlight the promise of BUD-SLNs as an effective oral drug delivery system capable of enhancing the solubility, stability, and potential bioavailability of budesonide. Further *in vivo* studies are reasonable to confirm these findings and explore clinical translation.

Declarations

Funding

The present work was supported by the Istanbul University Scientific Research Projects Coordination Unit. Project No: 39984.

Author Contribution

Conceptualization: M.M., B.D., Ö.A., N.N., Y.Ö.Methodology: M.M., B.D., Ö.A., N.N.Software: M.M., B.D.Validation: M.M., B.D.Formal analysis: M.M., B.D., Ö.A., N.N.Resources: M.M., B.D., Y.Ö.Writing – original draft preparation: M.M., B.D., Ö.A., N.N.Writing – review and editing: M.M., B.D., Y.Ö.Supervision: B.D., Y.Ö.Project administration: B.D., Y.Ö.Funding acquisition: Y.Ö.

Acknowledgement

The authors are also thankful to Suheung America Corporation for providing a gift sample of EMBOCAPS® AP (capsules). Though Özlem Akbal-Dağıstan is no longer with us, her light lives on in every line of this work and in our hearts.

References

1. Wang R, Li Z, Liu S, Zhang D. Global, regional and national burden of inflammatory bowel disease in 204 countries and territories from 1990 to 2019: a systematic analysis based on the Global Burden of Disease Study 2019. BMJ Open. 2023;13(3):e065186.
2. Rajput IB, Khan D, Mirza R, Ahmed N, Shah SU, Asad M, et al. Inflammatory Bowel Disease: Exploring Pathogenesis, Epidemiology, Conventional Therapies, and Advanced Nanoparticle Based Drug Delivery Systems. Bionanoscience. 2025;15(1):206.
3. Yagisawa K, Kubota A, Imai S, Nashimoto S, Sato Y, Kashiwagi H, et al. Actual Use of Budesonide Enteric-Coated Capsules for Crohn's Disease in Japan: Analysis of Health Insurance Big Data. Biol Pharm Bull. 2025;48(1):33–8.
4. Dolinger M, Torres J, Vermeire S. Crohn's disease. Lancet [Internet]. 2024;403(10432):1177–91. Available from: https://doi.org/10.1016/S0140-6736(23)02586-2
5. Ali HSM, Ahmed FH, Rawan B, Hamad A, Marey A, Yaser MA et al. Locally Acting Budesonide-Loaded Solid Self-Microemulsifying Drug Delivery Systems (SMEDDS) for Distal Ulcerative Colitis. Int J Nanomedicine [Internet]. 2024;19(null):11819–46. Available from: https://www.tandfonline.com/doi/abs/10.2147/IJN.S484277
6. Nyamba I, Sombie CB, Yabre M, Zime-Diawara H, Yameogo J, Ouedraogo S et al. Pharmaceutical approaches for enhancing solubility and oral bioavailability of poorly soluble drugs. Eur J Pharm Biopharm. 2024;114513.
7. Aggarwal K, Joshi S, Jindal P, Patel P, Das Kurmi B. Solid Lipid Nanoparticles: An Innovative Drug Delivery System for Enhanced Bioavailability and Targeted Therapy. AAPS PharmSciTech. 2025;26(6):186.
8. Ryu S, Jin M, Lee HK, Wang MH, Baek JS, Cho CW. Effects of lipid nanoparticles on physicochemical properties, cellular uptake, and lymphatic uptake of 6-methoxflavone. J Pharm Investig [Internet]. 2022;52(2):233–41. Available from: https://doi.org/10.1007/s40005-021-00557-5
9. Mesut B, Al-Mohaya M, Gholap AD, Yeşilkaya E, Das U, Akhtar MS, et al. Demystifying the potential of lipid-based nanocarriers in targeting brain malignancies. Naunyn Schmiedebergs Arch Pharmacol. 2024;397(12):9243–79.
10. Gonçalves LMD, Maestrelli F, Mannelli LC, Ghelardini C, Almeida AJ, Mura P. Development of solid lipid nanoparticles as carriers for improving oral bioavailability of glibenclamide. Eur J Pharm Biopharm [Internet]. 2016;102(16):41–50. Available from: http://dx.doi.org/10.1016/j.ejpb.2016.02.012
11. Nazief AM, Hassaan PS, Khalifa HM, Sokar MS, El-Kamel AH. Lipid-based gliclazide nanoparticles for treatment of diabetes: Formulation, pharmacokinetics, pharmacodynamics and subacute toxicity study. Int J Nanomed. 2020;15:1129–48.
12. Cirri M, Mennini N, Maestrelli F, Mura P, Ghelardini C, di Cesare Mannelli L. Development and in vivo evaluation of an innovative Hydrochlorothiazide-in Cyclodextrins-in Solid Lipid Nanoparticles formulation with sustained release and enhanced oral bioavailability for potential hypertension treatment in pediatrics. Int J Pharm [Internet]. 2017;521(1–2):73–83. Available from: http://dx.doi.org/10.1016/j.ijpharm.2017.02.022
13. Mishra V, Bansal KK, Verma A, Yadav N, Thakur S, Sudhakar K, et al. Solid lipid nanoparticles: Emerging colloidal nano drug delivery systems. Pharmaceutics. 2018;10(4):1–21.
14. Al-Mohaya M, Mesut B. Quality By Design Approach for Novel Drug Delivery Systems BT - Introduction to Quality by Design (QbD): From Theory to Practice. In: Jain NK, Bajwa N, editors. Singapore: Springer Nature Singapore; 2024. pp. 243–61. Available from: https://doi.org/10.1007/978-981-99-8034-5_10
15. ICH ICH. Q8 (R2) Pharmaceutical Development. ICH Q9 (quality risk Manag ICH Q. 2009;10.
16. Duarte JG, Duarte MG, Piedade AP, Mascarenhas-Melo F. Rethinking Pharmaceutical Industry with Quality by Design: Application in Research, Development, Manufacturing, and Quality Assurance. AAPS J [Internet]. 2025;27(4):96. Available from: https://doi.org/10.1208/s12248-025-01079-w
17. Dezani AB, Dezani TM, Ferreira JCF, Serra CH. dos R. Solubility evaluation of didanosine: a comparison between the equilibrium method and intrinsic dissolution for biopharmaceutics classification purposes. Brazilian J Pharm Sci. 2017;53:e16128.
18. USP-Solubility Measurements. <1236 > Solubility Measurements. Pharm Forum 2017, 43 (2).
19. Lindenberg M, Kopp S, Dressman JB. Classification of orally administered drugs on the World Health Organization Model list of Essential Medicines according to the biopharmaceutics classification system. Eur J Pharm Biopharm. 2004;58(2):265–78.
20. Elbahwy IA, Ibrahim HM, Ismael HR, Kasem AA. Enhancing bioavailability and controlling the release of glibenclamide from optimized solid lipid nanoparticles. J Drug Deliv Sci Technol [Internet]. 2017;38:78–89. Available from: http://dx.doi.org/10.1016/j.jddst.2017.02.001
21. Kamani P, Parikh K, Kapadia R, Sawant K. Phospholipid based ultra-deformable nanovesicular gel for transcutaneous application: QbD based optimization, characterization and pharmacodynamic profiling. J Drug Deliv Sci Technol. 2019;51:152–63.
22. Gupta S, Jhawat V. Quality by design (QbD) approach of pharmacogenomics in drug designing and formulation development for optimization of drug delivery systems. J Control Release. 2017;245:15–26.

23. Öztürk AA, Aygül A, Şenel B. Influence of glyceryl behenate, tripalmitin and stearic acid on the properties of clarithromycin incorporated solid lipid nanoparticles (SLNs): Formulation, characterization, antibacterial activity and cytotoxicity. J Drug Deliv Sci Technol [Internet]. 2019;54(May):101240. Available from: https://doi.org/10.1016/j.jddst.2019.101240
24. Sabir F, Katona G, Ismail R, Sipos B, Ambrus R, Csóka I. Development and characterization of N-propyl gallate encapsulated solid lipid nanoparticles-loaded hydrogel for intranasal delivery. Pharmaceuticals. 2021;14(7).
25. Zhao J, Liu Y, Shen C, Lai O-M, Tan C-P, Cheong L-Z. Enhanced storage stability and in-vitro digestibility of powdered-solid lipid nanoparticles with high-algae oil-load. Food Biosci. 2023;55:102810.
26. Alghananim A, Özalp Y, Mesut B, Serakinci N, Özsoy Y, Güngör S. A solid ultra fine self-nanoemulsifying drug delivery system (S-snedds) of deferasirox for improved solubility: Optimization, characterization, and in vitro cytotoxicity studies. Pharmaceuticals. 2020;13(8):1–25.
27. Mohamed RA, Abass HA, Attia MA, Heikal OA. Formulation and evaluation of metoclopramide solid lipid nanoparticles for rectal suppository. J Pharm Pharmacol. 2013;65(11):1607–21.
28. Mesut B, Sahin SHT, Ozsoy Y. Budesonide-Loaded Self-Nanoemulsion Formulations Optimisation and Characterisation Studies. Lat Am J Pharm. 2020;39(7):1368–78.
29. USP-NF. <1174 > Powder Flow. Stage 4 Harmon Off [Internet]. 2024; Available from: https://online.uspnf.com/uspnf/document/1_GUID-D48AA926-0912-4F7D-8B2B-3A022A1196FE_1_en-US
30. Nazlı H, Mesut B, Özsoy Y. In Vitro Evaluation of a Solid Supersaturated Self Nanoemulsifying Drug Delivery System (Super-SNEDDS) of Aprepitant for Enhanced Solubility. 2021;1–25.
31. RF H. A new approach for measurement of cytotoxicity using colorimetric assay. J Immunol Methods. 1993;160:89–96.
32. Anwer MK, Ahmed MM, Aldawsari MF, Alshahrani S, Fatima F, Ansari MN, et al. Eluxadoline loaded solid lipid nanoparticles for improved colon targeting in rat model of ulcerative colitis. Pharmaceuticals. 2020;13(9):1–16.
33. Beran K, Abrahamsson B, Charoo N, Cristofoletti R, Holm R, Kambayashi A, et al. Biowaiver monographs for immediate-release solid oral dosage forms: Voriconazole. J Pharm Sci. 2025;114(2):660–80.
34. Mesut B, Sahin SHT, Ozsoy Y. Budesonide self-nanoemulsion formulation as an oral drug delivery system: preparation, characterization and cytotoxicity studies. Pressacademia. 2017;5(1):41–6.
35. Kapadne C, Birari S, Gulecha V, Shinde A, Sambare A, Kshirsagar SK. Formulation and Evaluation of Budesonide-loaded Nanosponges for Colon-specific Drug Delivery Systems. BIO Integr. 2024;5(1):979.
36. Bhatt H, Naik B, Dharamsi A. Solubility Enhancement of Budesonide and Statistical Optimization of Coating Variables for Targeted Drug Delivery. J Pharm [Internet]. 2014;2014(1):262194. Available from: https://doi.org/10.1155/2014/262194
37. Tamer MA, Kassab HJ. Optimizing Intranasal Amisulpride Loaded Nanostructured Lipid Carriers: Formulation, Development, and Characterization Parameters. Pharm Nanotechnol. 2025;13(2):287–302.
38. Dahan A, Beig A, Lindley D, Miller JM. The solubility–permeability interplay and oral drug formulation design: Two heads are better than one. Adv Drug Deliv Rev [Internet]. 2016;101:99–107. Available from: https://www.sciencedirect.com/science/article/pii/S0169409X16301284
39. Smejkal G, Gross V, Lazarev A. Theoretical and Experimental Determinations of the Hydrophilic–Lipophilic Balance (HLB) of Representative Oils and Lecithins. Colloids Interfaces. 2024;8(2):21.
40. Park JH, Kim DS, Mustapha O, Yousaf AM, Kim JS, Kim DW et al. Comparison of a revaprazan-loaded solid dispersion, solid SNEDDS and inclusion compound: Physicochemical characterisation and pharmacokinetics. Colloids Surfaces B Biointerfaces [Internet]. 2018;162:420–6. Available from: https://www.sciencedirect.com/science/article/pii/S0927776517308573
41. Shevalkar G, Vavia P. Solidified nanostructured lipid carrier (S-NLC) for enhancing the oral bioavailability of ezetimibe. J Drug Deliv Sci Technol [Internet]. 2019;53(July):101211. Available from: https://doi.org/10.1016/j.jddst.2019.101211
42. Hussain A, Shakeel F, Singh SK, Alsarra IA, Faruk A, Alanazi FK, et al. Solidified SNEDDS for the oral delivery of rifampicin: Evaluation, proof of concept, in vivo kinetics, and in silico GastroPlusTM simulation. Int J Pharm. 2019;566:203–17.
43. Tan A, Rao S, Prestidge CA. Transforming lipid-based oral drug delivery systems into solid dosage forms: An overview of solid carriers, physicochemical properties, and biopharmaceutical performance. Pharm Res. 2013;30(12):2993–3017.
44. Patra CN, Singha R, Sahu K, Jena GK, Das NR, Sruti J. Current Updated Review on Applications of Different Grades of Sylysia in Pharmaceutical Formulation Development. Biomed Mater Devices [Internet]. 2025;3(1):415–32. Available from: https://doi.org/10.1007/s44174-024-00211-2
45. Lin Z, Zheng K, Azad MA, Davé RN. Preparation of Free-Flowing Spray-Dried Amorphous Composites Using Neusilin®. AAPS PharmSciTech [Internet]. 2023;24(1):51. Available from: https://doi.org/10.1208/s12249-023-02511-0
46. Aldosari BNA. Development and evaluation of self-nanoemulsifying drug delivery systems for oral delivery of indomethacin [Internet]. UCL (University College London); 2018. Available from: https://discovery.ucl.ac.uk/id/eprint/10044225
47. Djuris J, Ibric S, Đurić Z. Chapter 1 - Quality by design in the pharmaceutical development. In: Djuris JBT-C-AA in PT (Second E, editor. Woodhead Publishing Series in Biomedicine [Internet]. Woodhead Publishing; 2024. pp. 1–21. Available from: https://www.sciencedirect.com/science/article/pii/B9780443186554000030
48. Gurumukhi VC, Bari SB. Fabrication of efavirenz loaded nano-formulation using quality by design (QbD) based approach: Exploring characterizations and in vivo safety. J Drug Deliv Sci Technol [Internet]. 2020;56(November 2019):101545. Available from: https://doi.org/10.1016/j.jddst.2020.101545
49. Bandi SP, Kumbhar YS, Venuganti VVK. Effect of particle size and surface charge of nanoparticles in penetration through intestinal mucus barrier. J Nanoparticle Res [Internet]. 2020;22(3):62. Available from: https://doi.org/10.1007/s11051-020-04785-y

50. Rehman M, Tahir N, Sohail MF, Qadri MU, Duarte SOD, Brandão P, et al. Lipid-based nanoformulations for drug delivery: An ongoing perspective. Pharmaceutics. 2024;16(11):1376.
51. Al-Mohaya M, Çelik YS, Demiralp B. Chapter 15 - Evaluation of lipid-based formulation for pulmonary delivery. In: Faiyazuddin MD, Ali H, Akbar MD, Iqbal BBT-L in PDD, editors. Academic Press; 2025. pp. 337–52. Available from: https://www.sciencedirect.com/science/article/pii/B9780443223747000153
52. Mussi SV, Silva RC, de Oliveira MC, Lucci CM, de Azevedo RB, Ferreira LAM. New approach to improve encapsulation and antitumor activity of doxorubicin loaded in solid lipid nanoparticles. Eur J Pharm Sci [Internet]. 2013;48(1):282–90. Available from: https://www.sciencedirect.com/science/article/pii/S0928098712004289
53. Salminen H, Kasapoğlu KN, Özçelik B, Weiss J. Stabilization of solid lipid nanoparticles with glycyrrhizin. Eur Food Res Technol [Internet]. 2023;249(3):787–98. Available from: https://doi.org/10.1007/s00217-022-04176-8
54. Nooli M, Chella N, Kulhari H, Shastri NR, Sistla R. Solid lipid nanoparticles as vesicles for oral delivery of olmesartan medoxomil: formulation, optimization and in vivo evaluation. Drug Dev Ind Pharm [Internet]. 2017;43(4):611–7. Available from: http://dx.doi.org/10.1080/03639045.2016.1275666
55. Nazarova A, Yakimova L, Filimonova D, Stoikov I. Surfactant Effect on the Physicochemical Characteristics of Solid Lipid Nanoparticles Based on Pillar[5]arenes. 23, Int J Mol Sci. 2022.
56. Burapapadh K, Takeuchi H, Sriamornsak P. Novel pectin-based nanoparticles prepared from nanoemulsion templates for improving in vitro dissolution and in vivo absorption of poorly water-soluble drug. Eur J Pharm Biopharm. 2012;82(2):250–61.
57. Joseph E, Reddi S, Rinwa V, Balwani G, Saha R. Design and in vivo evaluation of solid lipid nanoparticulate systems of Olanzapine for acute phase schizophrenia treatment: Investigations on antipsychotic potential and adverse effects. Eur J Pharm Sci [Internet]. 2017;104:315–25. Available from: http://dx.doi.org/10.1016/j.ejps.2017.03.050
58. Chettupalli AK, Bukke SPN, Rahaman SA, Unnisa A, Adepu M, Kavitha M et al. Ritonavir loaded solid lipid nanoparticles for oral drug delivery and bioavailability enhancement. Discov Appl Sci [Internet]. 2025;7(1):58. Available from: https://doi.org/10.1007/s42452-024-06322-1
59. Mir MA, Akhter MH, Afzal O, Rab SO, Altamimi ASA, Alossaimi MA et al. Design-of-Experiment-Assisted Fabrication of Biodegradable Polymeric Nanoparticles: In Vitro Characterization, Biological Activity, and In Vivo Assessment. ACS Omega [Internet]. 2023;8(42):38806–21. Available from: https://doi.org/10.1021/acsomega.3c01153
60. Smith MC, Crist RM, Clogston JD, McNeil SE. Zeta potential: a case study of cationic, anionic, and neutral liposomes. Anal Bioanal Chem. 2017;409:5779–87.
61. Clogston JD, Patri AK. Zeta Potential Measurement BT - Characterization of Nanoparticles Intended for Drug Delivery. In: McNeil SE, editor. Totowa, NJ: Humana Press; 2011. pp. 63–70. Available from: https://doi.org/10.1007/978-1-60327-198-1_6
62. Slavkova M, Lazov C, Spassova I, Kovacheva D, Tibi IP, Stefanova D et al. Formulation of Budesonide-Loaded Polymeric Nanoparticles into Hydrogels for Local Therapy of Atopic Dermatitis. Vol. 10, Gels. 2024.
63. Lopes CE, Langoski G, Klein T, Ferrari PC, Farago PV. A simple HPLC method for the determination of halcinonide in lipid nanoparticles: development, validation, encapsulation efficiency, and in vitro drug permeation. Brazilian J Pharm Sci. 2017;53(2):e15250.
64. Vijayakumar A, Baskaran R, Jang YS, Oh SH, Yoo BK. Quercetin-Loaded Solid Lipid Nanoparticle Dispersion with Improved Physicochemical Properties and Cellular Uptake. AAPS PharmSciTech [Internet]. 2017;18(3):875–83. Available from: http://dx.doi.org/10.1208/s12249-016-0573-4
65. Goyanes A, Chang H, Sedough D, Hatton GB, Wang J, Buanz A et al. Fabrication of controlled-release budesonide tablets via desktop (FDM) 3D printing. Int J Pharm [Internet]. 2015;496(2):414–20. Available from: https://www.sciencedirect.com/science/article/pii/S0378517315303082
66. Fülöpová N, Pavloková S, DeBono I, Vetchý D, Franc A. Development and Comparison of Various Coated Hard Capsules Suitable for Enteric Administration to Small Patient Cohorts. Vol. 14, Pharmaceutics. 2022.
67. Dressman J. Comparative dissolution of budesonide from four commercially available products for oral administration: implications for interchangeablity. Dissolution Technol. 2023;30(4):224–9.
68. Campos JR, Severino P, Santini A, Silva AM, Shegokar R, Souto SB et al. Chapter 1 - Solid lipid nanoparticles (SLN): prediction of toxicity, metabolism, fate and physicochemical properties. In: Shegokar RBT-N, editor. Elsevier; 2020. pp. 1–15. Available from: https://www.sciencedirect.com/science/article/pii/B9780128177785000014
69. Beloqui A, Solinís MÁ, Rodríguez-Gascón A, Almeida AJ, Préat V. Nanostructured lipid carriers: Promising drug delivery systems for future clinics. Nanomedicine Nanotechnology, Biol Med [Internet]. 2016;12(1):143–61. Available from: http://dx.doi.org/10.1016/j.nano.2015.09.004

Tables

Table 1

Solubility results of 9 mg BUD in different media at 37°C (mean ± SD, n = 3).

Dose (D) (mg)	Media	Solubility (S) (mg/mL) ± SD	D/S Ratio (mL)	D_0
9	1.2	0.027(± 0.09)	324	1.29
	4.5	0.027(± 0.04)	324	1.29
	6.8	0.024(± 0.06)	362	1.45
	*FaSSIF	-	-	-
	*FeSSIF	-	-	-

Table 2

CQAs of BUD-SLNs.

CQAs of final product	Target	Is it a CQA?	Justification(s)
Physical Attributes	Appearance acceptable to the patient with odorless	No	Appearance and odor do not directly affect the performance of SLNs. Also, Appearance and odor are not directly linked to safety and efficacy.
Particle Size	< 200 nm	Yes	Smaller particle size enhances dissolution and results in permeation through gastrointestinal epithelial cell lining, which can influence on safety and efficacy.
Polydispersity Index	< 0.2	Yes	It indicates a narrow particle size distribution, which can influence dissolution results.
Zeta Potential	Higher than + 30 mV or less than − 30 mV	No	Zeta potential is necessary for maintaining the stability of the system.
Entrapment Efficiency	> 90%	Yes	Maximum value of entrapment efficiency is essential, which can influence therapeutic effect directly.
Dissolution: According to FDA, Acid stage: 0.1 N HCl 2 h, 1000ml Phosphate buffer: pH 7.5, 1000ml for 8 h in USP II (Paddle, 75 rpm) apparatus	Acid stage: No release Buffer stage: According to (29), NLT 75%	Yes	It indicates drug release from SLNs in ileum targeting, which can influence safety and efficacy directly.

Table 3

Levels of independent variables and constraints of responses.

Independent variables	Levels				
	Low (-1)		High (+ 1)		
X_1= Lipid concentration (Cetyl stearyl alcohol, %)	10		15		
X_2= Surfactant concentration (Cremophor® A25, %)	0		5		
X_3= Surfactant concentration (Gelucire® 44/14, %)	0		5		
X_4= Homogenization time (min)	10		20		
Dependent variables	Condition	Objective	Minimum	Target	Maximum
Y_1= Particle size (nm)	Required	Minimize	-	100	200
Y_2 = Polydispersity index	Required	Minimize	-	0.2	0.25
Y_3= Entrapment efficiency (EE%)	Required	Maximize	70	90	100
Y_4 = Cumulative drug release after 2 h (%)	Required	Maximize	75	90	100

Table 4

Experimental design of the prepared BUD-SLNs formulations and correspondent characterization parameters (mean ± SD, n = 3).

Run	Factors (Independent variables)				Responses (Dependent variables)			
	Lipid concentration (CSA, %) (X_1)	Surfactant concentration (CA25, %) (X_2)	Surfactant concentration (G44, %) (X_3)	HT (min) (X4)	PS (nm) (Y1)	PDI (Y2)	EE (%) (Y3)	Cumulative drug release after 2 h (%) (Y_4)
9	10	0	0	20	10.64 ± 0.60	0.170 ± 0.06	99.80 ± 0.01	96.49 ± 4.79
1	10	0	0	10	10.34 ± 0.16	0.188 ± 0.06	99.81 ± 0.02	104.52 ± 3.96
7	10	5	5	10	10.55 ± 0.08	0.107 ± 0.01	99.84 ± 0.23	102.59 ± 2.28
5	10	0	5	10	16.30 ± 0.05	0.240 ± 0.02	99.79 ± 0.03	91.83 ± 3.40
13	10	0	5	20	10.62 ± 0.05	0.082 ± 0.03	99.78 ± 0.1	97.91 ± 3.05
3	10	5	0	10	10.10 ± 0.08	0.069 ± 0.02	99.80 ± 0.01	101.63 ± 2.23
15	10	5	5	20	10.49 ± 0.02	0.098 ± 0.01	99.82 ± 0.1	58.48 ± 7.78
11	10	5	0	20	10.24 ± 0.04	0.088 ± 0.02	99.81 ± 0.03	94.87 ± 5.12
18	10	2.5	2.5	15	10.73 ± 0.05	0.136 ± 0.03	99.78 ± 0.01	86.48 ± 0.96
17	12.5	2.5	2.5	15	11.09 ± 0.10	0.254 ± 0.02	99.86 ± 0.00	106.87 ± 4.73
21	12.5	5	2.5	15	10.43 ± 0.06	0.168 ± 0.02	99.86 ± 0.04	67.43 ± 9.77
22	12.5	2.5	0	15	10.13 ± 0.04	0.074 ± 0.01	99.78 ± 0.01	89.18 ± 5.57
24	12.5	2.5	2.5	10	11.20 ± 0.14	0.250 ± 0.02	99.78 ± 0.50	102.6 ± 7.55
25	12.5	2.5	2.5	20	54.90 ± 68.9	0.187 ± 0.05	99.85 ± 0.12	105.2 ± 3.42
23	12.5	2.5	5	15	10.57 ± 0.06	0.108 ± 0.02	99.81 ± 0.01	96.62 ± 4.67
27	12.5	2.5	2.5	15	10.68 ± 0.20	0.195 ± 0.02	99.86 ± 0.00	106.05 ± 3.26
26	12.5	2.5	2.5	15	10.85 ± 0.14	0.212 ± 0.03	99.86 ± 0.00	95.21 ± 1.87
20	12.5	0	2.5	15	10.33 ± 0.04	0.081 ± 0.01	99.92 ± 0.04	55.78 ± 4.99
6	15	0	5	10	10.48 ± 0.07	0.105 ± 0.01	99.83 ± 0.05	114.04 ± 6.20
4	15	5	0	10	10.15 ± 0.12	0.104 ± 0.01	99.80 ± 0.01	98.53 ± 2.30
14	15	0	5	20	10.57 ± 0.04	0.167 ± 0.01	99.92 ± 0.07	116.91 ± 8.70
2	15	0	0	10	10.06 ± 0.04	0.091 ± 0.02	99.78 ± 0.01	101.54 ± 0.75
16	15	5	5	20	-	-	-	-
12	15	5	0	20	10.55 ± 0.06	0.162 ± 0.02	99.79 ± 0.02	81.2 ± 1.92
10	15	0	0	20	10.15 ± 0.02	0.090 ± 0.01	99.78 ± 0.01	109.78 ± 9.53
8	15	5	5	10	-	-	-	-

Run	Factors (Independent variables)				Responses (Dependent variables)			
	Lipid concentration (CSA, %) (X_1)	**Surfactant concentration (CA25, %) (X_2)**	**Surfactant concentration (G44, %) (X_3)**	**HT (min) (X4)**	**PS (nm) (Y1)**	**PDI (Y2)**	**EE (%) (Y3)**	**Cumulative drug release after 2 h (%) (Y_4)**
19	15	2.5	2.5	15	10.31 ± 0.03	0.123 ± 0.02	99.83 ± 0.08	106.24 ± 9.90

Table 5

Actual values and predicted values for all dependent variables of the optimized formulation, along with their P-values (mean ± SD

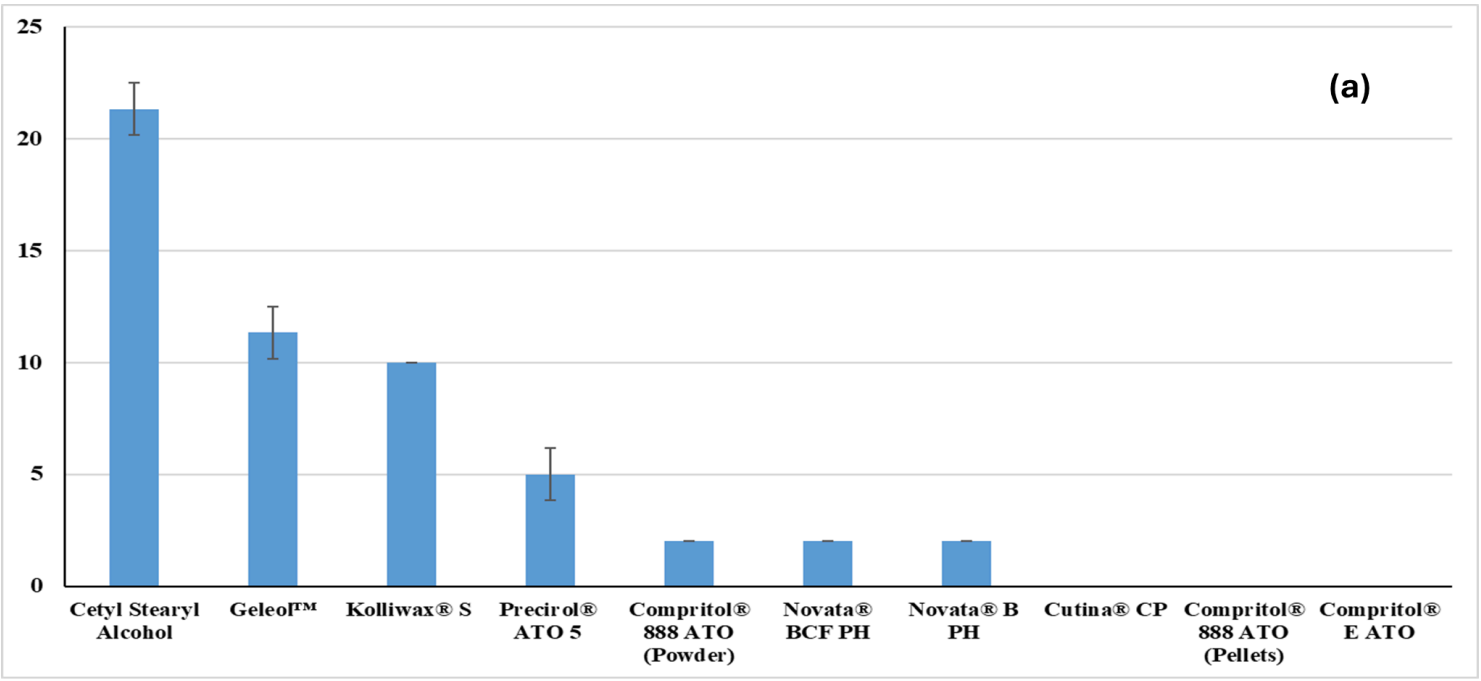
Run	Factors (Independent variables)				Actual Value				Predicted value				P-v
					Responses (Dependent variables)				Responses (Dependent variables)				
	Lipid concentration (CSA, %) (X1)	Surfactant concentration (CA25, %) (X2)	Surfactant concentration (G44, %) (X3)	HT (min) (X4)	PS (nm) (Y1)	PDI (Y2)	EE% (Y3)	Cumulative drug release after 2 h (%) (Y_4)	PS (nm) (Y1)	PDI (Y2)	EE% (Y3)	Cumulative drug release after 2 h (%) (Y_4)	PS (nm) (Y
4	15	5	0	10	10.15 ± 0.12	0.104 ± 0.01	99.80 ± 0.01	98.53 ± 2.30	9.5 ± 1.15	0.088 ± 0.03	99.80 ± 0.01	97.93 ± 8.3	0.4

Table 6

Stability studies of optimized BUD-SLNs.

25 ± 2°C/65 ± 5% RH				
Months	**PS (nm)**	**PDI**	**EE (%)**	**Cumulative drug release after 2 h (%)**
0	10.15 ± 0.12	0.104 ± 0.01	99.80 ± 0.01	98.53 ± 2.30
1	11.00 ± 0.01	0.126 ± 0.01	99.30 ± 0.04	98.32 ± 3.02
2	11.92 ± 0.08	0.162 ± 0.02	99.30 ± 0.02	97.45 ± 2.51
3	12.15 ± 0.06	0.189 ± 0.01	99.20 ± 0.01	97.08 ± 4.67
40 ± 2°C/75 ± 5% RH				
Months	PS (nm)	PDI	EE (%)	Cumulative drug release after 2 h (%)
0	10.15 ± 0.12	0.104 ± 0.01	99.80 ± 0.01	98.53 ± 2.30
1	11.56 ± 0.07	0.150 ± 0.09	99.50 ± 0.00	98.00 ± 2.79
2	11.80 ± 0.10	0.175 ± 0.01	99.20 ± 0.01	97.05 ± 3.48
3	12.82 ± 0.04	0.191 ± 0.04	99.00 ± 0.02	96.98 ± 3.91

Figures



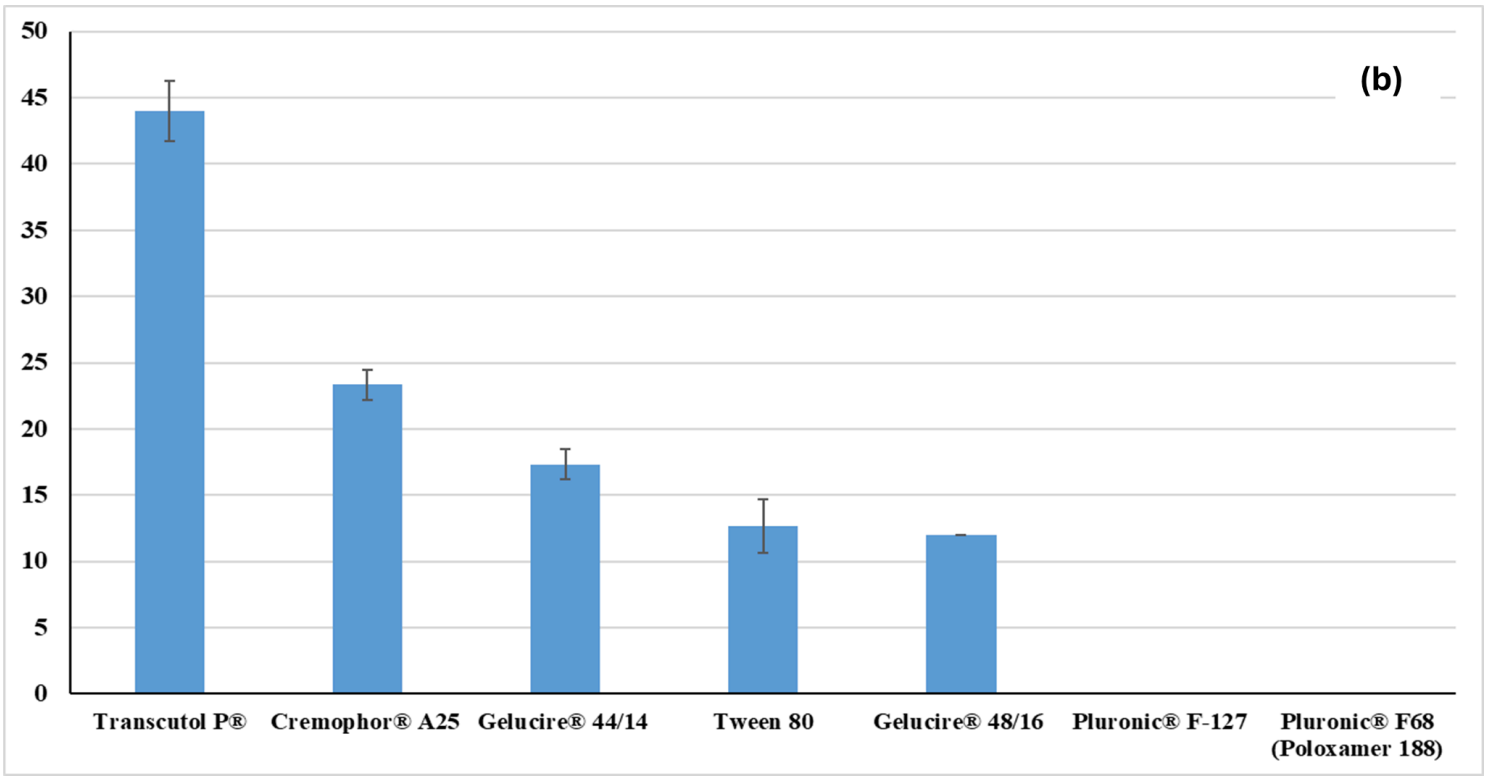


Figure 1

Solubility studies of BUD in various a) solid lipids, (b) surfactants (mg/g) (mean±SD, n=3).

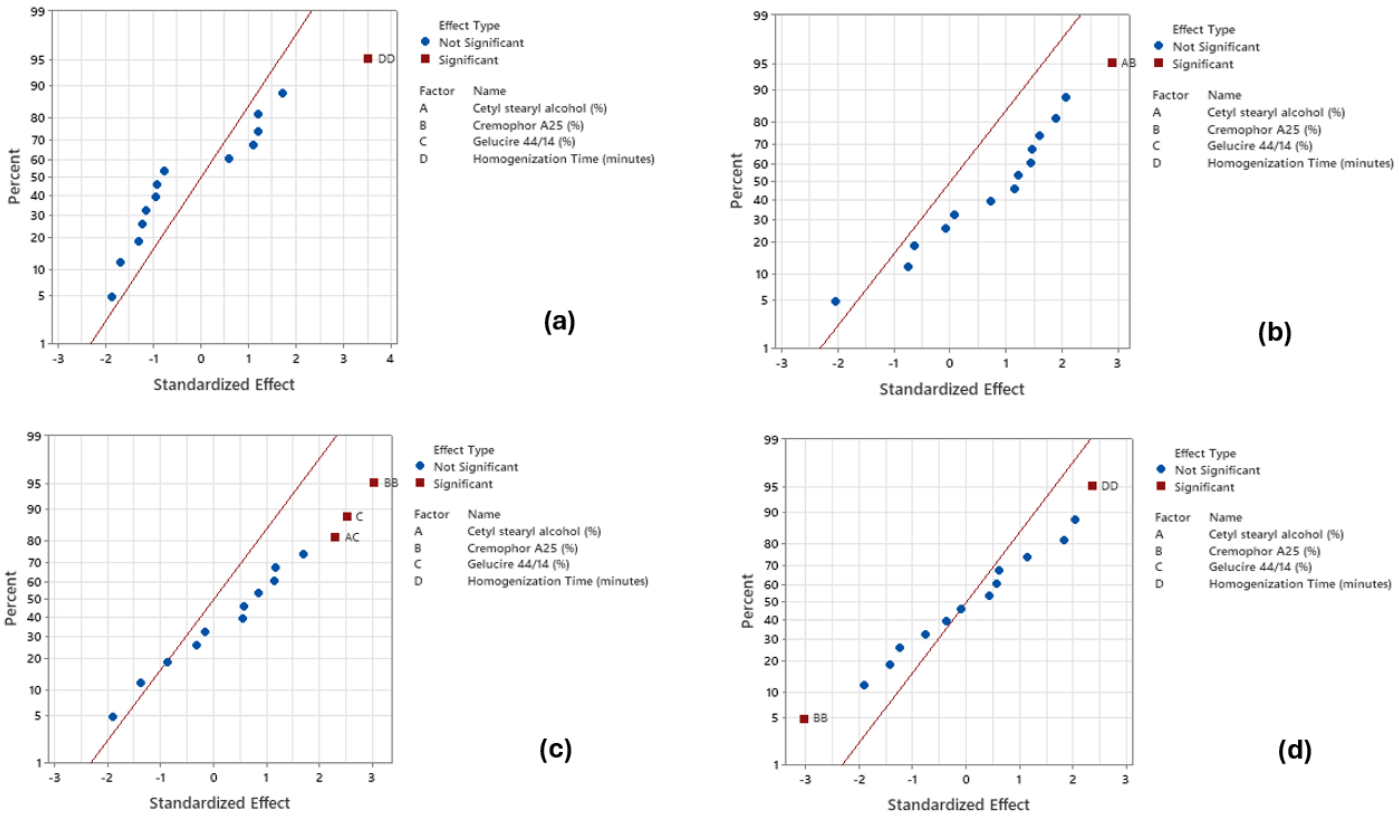


Figure 2

Normal plot of standardized effects for (a) PS, (b) PDI, (c) EE%, and (d) Cumulative drug release after 2 hours.

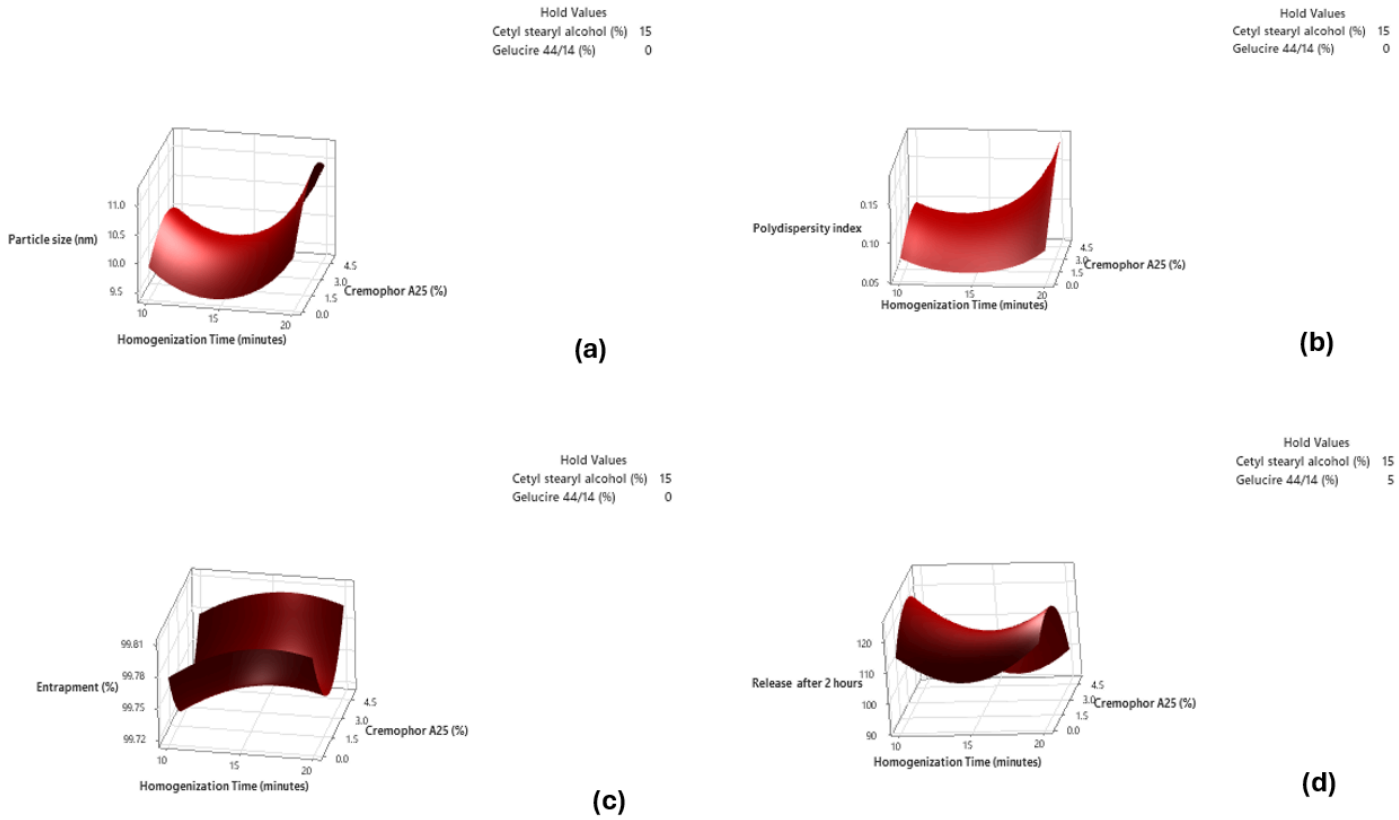


Figure 3

Surface plots for (a) PS, (b) PDI, (c) EE%, and (d) Cumulative drug release after 2 hours.

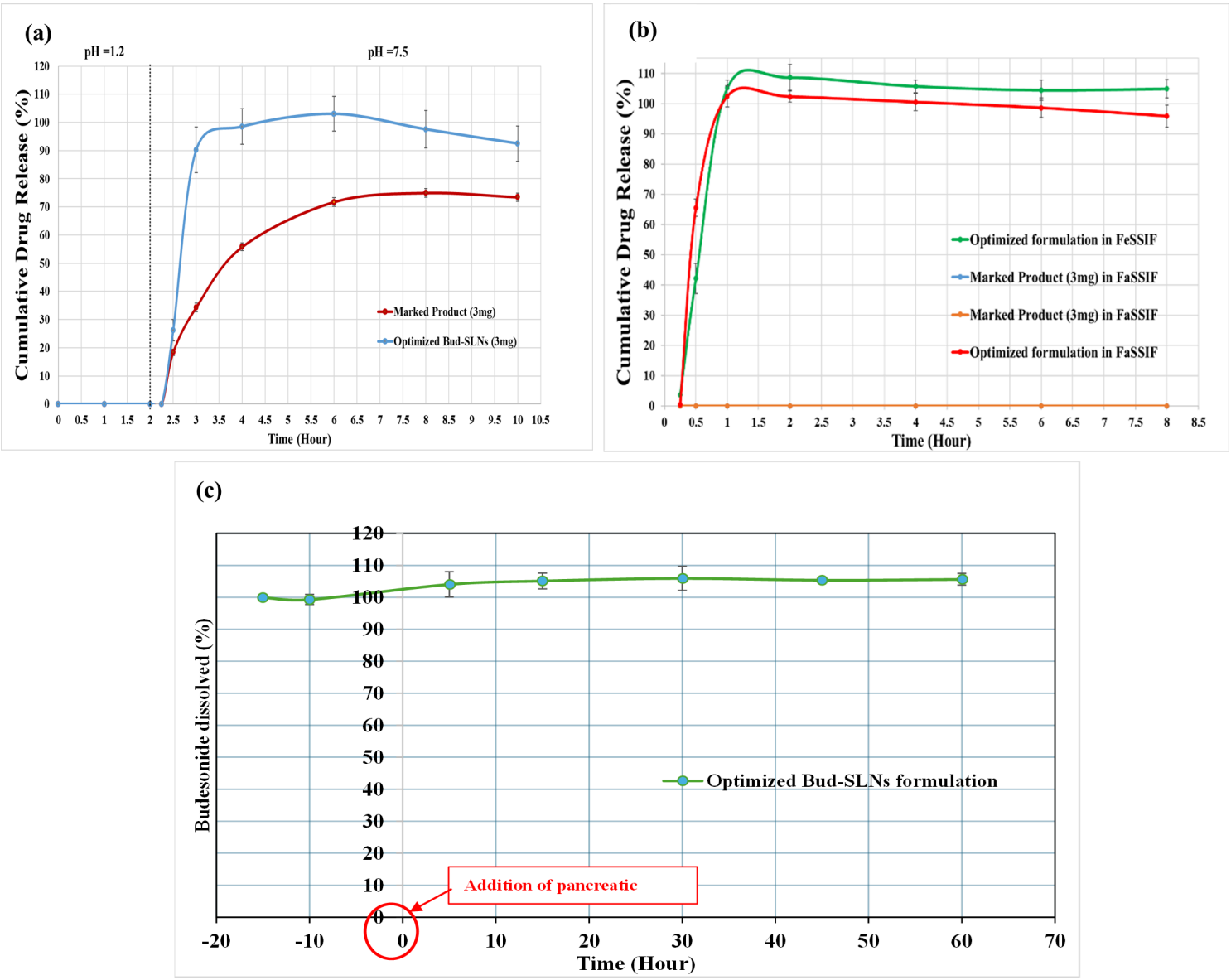


Figure 4

(a) Dissolution profiles in acidic (pH=1.2) and phosphate buffer (pH=7.5) medium, (b) Dissolution profiles in FaSSIF/FeSSIF medium of optimized BUD-SLNs and marked product (mean±SD, n=3) (The blue line is parallel and below the orange line in FaSSIF/FeSSIF medium), (c) *In vitro* lipolysis performance study of optimized BUD-SLNs formulation.

Supplementary Files

This is a list of supplementary files associated with this preprint. Click to download.

- SupplementaryMM1.docx